Published in final edited form as:
Pflugers Arch. 2013 July ; 465(7): 997–1010. doi:10.1007/s00424-013-1224-1.

Characterization of distinct single-channel properties of Ca^{2+} inward currents in mitochondria

Alexander I. Bondarenko, **Claire Jean-Quartier**, **Roland Malli**, and **Wolfgang F. Graier**
Institute of Molecular Biology and Biochemistry, Center of Molecular Medicine, Medical University of Graz, Harrachgasse 21/III, 8010 Graz, Austria

Abstract

Previous studies have demonstrated several molecularly distinct players involved in mitochondrial Ca^{2+} uptake. In the present study, electrophysiological recordings on mitoplasts that were isolated from HeLa cells were performed in order to biophysically and pharmacologically characterize Ca^{2+} currents across the inner mitochondrial membrane. In mitoplast-attached configuration with 105 mM Ca^{2+} as a charge carrier, three distinct channel conductances of 11, 23, and 80 pS were observed. All types of mitochondrial currents were voltage-dependent and essentially depended on the presence of Ca^{2+} in the pipette. The 23 pS channel exhibited burst kinetics. Though all channels were sensitive to ruthenium red, their sensitivity was different. The 11 and 23 pS channels exhibited a lower sensitivity to ruthenium red than the 80 pS channel. The activities of all channels persisted in the presence of cylosporin A, CGP 37187, various K^+-channel inhibitors, and Cl^- channel blockers disodium 4,4′-diisothiocyanatostilbene-2,2′-disulfonate and niflumic acid. Collectively, our data identified multiple conductances of Ca^{2+} currents in mitoplasts isolated from HeLa cells, thus challenging the dogma of only one unique mitochondrial Ca^{2+} uniporter.

Keywords

Mitochondrial Ca^{2+} channels; Mitoplast; Mitochondria; Ca^{2+} signaling; Patch clamp

Introduction

Mitochondrial functions largely depend on their ability to take up, accumulate and release Ca^{2+}. Thus, mitochondrial Ca^{2+} homeostasis is of pivotal importance for the functions of the organelle as well as the cellular Ca^{2+} signaling and function (for review, see [7, 9]). Isolated mitochondria can rapidly take up a large amounts of Ca^{2+} in a mitochondrial membrane potential-dependent manner via the Ca^{2+} uniporter pathway [14]. Although the mystery of the nature of the mitochondrial Ca^{2+} uniporter has been enlightened by the identification of the so-called mitochondrial Ca^{2+} uniporter (MCU) [3, 6] and its regulator and gatekeeper the mitochondrial calcium uptake 1 (MICU1) [15, 19], our understanding on the properties and characteristics of mitochondrial Ca^{2+} uptake is limited. In a landmark publication, the group of David Clapham described a Ca^{2+} entry current in isolated mitoplasts of which the biophysical characteristics (e.g., ion selectivity and sensitivity) fulfill the features expected from the mitochondrial Ca^{2+} uniporter channel [13]. In another study performed on rat heart

wolfgang.graier@medunigraz.at.

Europe PMC Funders Author Manuscripts

mitochondria, four distinct Ca^{2+} channel conductances that were established by mitochondrial ryanodine receptor type 1 (RYR1) were identified [21, 22]. Moreover, the leucine zipper EF hand-containing transmembrane protein 1 (LETM 1) was also described as a putative Ca^{2+} carrier in the inner mitochondrial membrane [12]. Under certain conditions mitochondrial Na^{+}–Ca^{2+} exchanger (NCX_{mito}) and the novel uncoupling proteins 2 and 3 (UCP2/3) were shown to accomplish the transfer of Ca^{2+} across the inner mitochondrial membrane [26, 27, 29], thus, emphasizing the existence of multiple mitochondrial Ca^{2+} uptake routes. In line with this consideration, more recently, single-channel patch clamp recordings from cardiac mitochondria revealed two different Ca^{2+} channels with distinct gating properties and sensitivity to Ru360 [17], thus questioning the dogma of the existence of one unique channel that exclusively accounts for mitochondrial Ca^{2+} uptake. Notably, distinct Ca^{2+} channels in the inner mitochondrial membrane of one given mitochondrion is not specific for cardiac mitochondria. In our previous work, we described two and three Ca^{2+} inward currents in mitoplasts form HeLa and endothelial cells, respectively [11]. Accordingly, the dogma of a unique and ubiquitously established Ca^{2+} flux through the inner mitochondrial membrane is challenged and the existence of multiple Ca^{2+} entry routes/modes that establish distinct Ca^{2+} currents in one given mitochondria has to be considered.

Notably, a biophysical and pharmacological characterization of these distinct but coexisting Ca^{2+} currents through the inner membrane of mitochondria is missing whilst fundamental for future studies that aim to investigate the individual contribution of the putative candidate proteins (MCU [3, 6], RyR1 [22], LETM 1 [12, 28], and UCP2/3 [25, 26]) that actually accomplish mitochondrial Ca^{2+} uptake. Accordingly, this study was designed to characterize single-channel Ca^{2+} currents in mitoplasts isolated from HeLa cells and to describe the individual biophysical and pharmacological properties of distinct mitochondrial Ca^{2+} channels.

Materials and methods

Cell culture and isolation of mitochondria

HeLa cells were grown on DMEM containing 10 % FCS, 50 U/ml penicillin and 50 μg/ml streptomycin. Mitochondria were freshly isolated as previously described [11] with some modifications. Mitochondria were prepared from HeLa cells by differential centrifugation. Cells were trypsinized, harvested, and washed with PBS. All consecutive steps were carried out at 4 °C according to the protocol described by Frezza et al. [8]. The cell pellet was suspended in a 200-mM sucrose buffer containing 10 mM Tris-MOPS, 1 mM EGTA and protease inhibitor (1:50, P8340 Sigma, Vienna, Austria; pH adjusted to 7.4 with Tris) and homogenized with a glass–Teflon potter (40–50 strokes). Nuclear remnants and cell debris were centrifuged down at 900×*g* for 10 min. Supernatant was centrifuged at 3,000×g for 20 min. The mitochondrial pellet was washed again with IMBc and centrifuged down at 7,000×*g* for 15 min. All fractions were kept on ice until further utilization.

Preparation of mitoplasts

Mitoplast formation was achieved by incubation of isolated mitochondria in hypotonic solution (5 mM HEPES, 5 mM sucrose, and 1 mM EGTA and pH adjusted to 7.4 with KOH) for 8–10 min. Then hypertonic solution (750 mM KCl, 80 mM HEPES, and 1 mM EGTA and pH adjusted to 7.4 with KOH of <10 mM) was added to restore isotonicity. Mitochondrial swelling was monitored as a change of optical density at 540 nm (Schott instruments UviLine 9400) [4, 10, 20]. Isolated mitoplasts appeared as transparent vesicles with attached remnants of the outer membrane. Purity of isolated mitochondria was verified by Western blots labeling plasma membrane and mitochondrial-localized proteins (Orai-1

(H-46:sc-68895 Santa Cruz, Szabo, Vienna, Austria and PSI-1819, Pro-Sci, Szabo, Vienna, Austria) and MCU (E-16:sc-246072 Santa Cruz), respectively).

Mitoplast patch clamp recordings

All measurements were performed in the mitoplast-attached configuration at room temperature. Patch pipettes were pulled from glass capillaries using a Narishige puller (Narishige Co., Ltd., Tokyo, Japan), fire-polished and had a resistance of 8–12 MΩ. Experimental buffers contained 105 mM $CaCl_2$ and 10 mM HEPES (pipette solution 1 (PS1)), or low chloride solution with 65 mM Ca-methanesulfonate, 40 mM $CaCl_2$, and 10 mM HEPES (PS2), both pH adjusted to 7.2 with $Ca(OH)_2$. Ca^{2+}-free pipette solution contained (in millimolars): 220 sucrose, 35 *N*-methyl-D-glucamine chloride, 2 EGTA, and 0.1 disodium 4,4′-diisothiocyanatostilbene-2,2′-disulfonate (DIDS; PS3) (Table 1). Bath solution contained 150 mM KCl, 1 mM EGTA, 1 mM EDTA, and 10 mM HEPES, pH was adjusted to 7.2 with KOH. If not otherwise indicated, all pipette solutions contained 10 μM Cyclosporin A (Tocris Bioscience, Bristol, UK) and 10 μM 7-chloro-5-(2-chlorophenyl)-1,5-dihydro-4,1-benzothiazepin-2(3H)-one (CGP 37187, Ascent Scientific Ltd., Bristol, UK) to prevent opening of the permeability transition pore (PTP) and the activity of the mitochondrial Na^+/Ca^{2+} exchanger (NCX_{mito}) as well as LETM1 [12], respectively. Ruthenium red (RuR; 1–30 μM; Merck Chemicals Ltd., Darmstadt, Germany) and DIDS (100 μM) were added as indicated. Currents were recorded using a patch-clamp amplifier (EPC7, List Electronics, Darmstadt, Germany). Data collection was performed using Clampex software of pClamp (V9.0, Axon Instruments). Signals obtained were low pass filtered at 1 kHz using an eight-pole Bessel filter (Frequency Devices), and digitized with a sample rate of 10 kHz using a Digidata 1200A A/D converter (Axon Instruments, Foster City, CA). Voltage ramps of 1 s duration from −150 to + 50 mV were delivered every 10 s from the holding potential 0 mV. Single-channel currents were recorded at a fixed holding potential indicated in the respective figures.

Results

Control of mitoplast preparation

To adjust optimal time of mitochondria incubation in hypotonic medium during mitoplast preparation, we monitored time-dependency of mitochondria swelling. Incubation in hypotonic solution resulted in a gradual decline of the optical density within 8–10 min (Fig. 1), which corresponds to mitochondria swelling and the start of outer membrane rupture and formation of mitoplast [4, 10, 20]. Mitochondria swelling reached a plateau phase within 10 to 20 min, which was followed by a gradual restoration in optical density. Accordingly, for mitoplast preparation from HeLa cells, isolated mitochondria were incubated in hypotonic solution for 7–8 min.

The plasma membrane is comprised of various Ca^{2+} channels that might interfere in our electrophysiological recordings with mitoplasts Ca^{2+} currents. Therefore, in order to assess a potentially contamination of the prepared mitoplasts, we tested for putative plasma membrane particles inside the mitochondrial fraction using Western Blotting. We tested the protein content within organelle fractions for Calcium release-activated calcium channel protein 1 (ORAI-1), as representative plasma membrane protein, and MCU as mitochondrial control protein. Densitometric analyses revealed a 3-fold increase of MCU content in mitochondrial fractions compared with whole cell lysates. Orai-1 was inconsistently present in mitochondrial fractions in approximately 20 times lower amount than in whole cell lysates. Prior electrophysiological measurements, mitoplasts were allowed to settle down to the glass bottom of the recording chamber, gently washed with bath solution, visualized and approached by the patch pipette.

Europe PMC Funders Author Manuscripts

Biophysical characterization of three distinct Ca^{2+} currents in mitoplasts

Recordings in the mitoplast-attached configuration with the use of high Ca^{2+}-containing pipette solution (PS1, Table 1) at test potentials from −100 to −150 mV in high K^+ bath solution revealed several types of single-channel activities. Based on the individual channel conductance and kinetics three distinct Ca^{2+} currents could be discriminated that were observed frequently in the same patch. The most predominant current was a 11.7±0.6-pS (n=14) channel that was referred to as intermediate mitochondrial Ca^{2+} channel (*i*-MCC) according to our previous report [11]. In high Ca^{2+}-containing pipette solution (PS1) *i*-MCC was found in about 70 % of patches. Figure 2a shows individual traces of the single-channel activity of *i*-MCC in a patch held at −100 mV. The channel did not inactivate over time during stepwise voltage shifts. Generally, more than one active channel was present in the patches. The corresponding amplitude histogram indicates the mean single-channel amplitude at −100 mV is approximately 1 pA (Fig. 2b). Representative traces of *i*-MCC channel at voltages −60 to −140 mV are shown in Fig. 2c. The channel activity starts noticeable at −60 mV. Shifting the holding potential towards more negative values gradually increased the single-channel activity (NPo) and amplitude that showed no rectification at potentials from −60 to −140 mV (Fig. 2d). Because of general instability of patches at voltages more negative than −140 mV in our experiments, we were unable to routinely investigate the channel behavior at −160 mV.

Under our standard experimental conditions (PS1), in 12 % of experiments a high conductance (60–100 pS) single-channel activity with a mean conductance of 80.2±7.8 pS (n=7) was observed that occurred in addition to the 11 pS *i*-MCC channel. The channel is characterized by a relatively long-lived open state, during which the channel exhibited bursting behavior. In line with our previous observation [11], this channel is referred to as the extra large conductance mitochondrial Ca^{2+} channel (*xl*-MCC). Representative traces of the channel activity at −100 mV and the corresponding amplitude histogram are shown in Fig. 3a, b. Generally, only one *xl*-MCC channel was present in one given patch, thus, pointing to a far lower density of this channel compared with *i*-MCC. During voltage steps, the *xl*-MCC channel activity tends to inactivate over time (Fig. 3a) and average of individual traces from the same patch is shown in Fig. 3c. The *xl*-MCC activity was observed either as a sole Ca^{2+} conductance in the patch (Fig. 3a) or together with *i*-MCC (Fig. 3d). The activity of xl-MCC started noticeable at −50 mV (Fig. 4a). Similar to *i*-MCC, single-channel amplitude of *xl*-MCC channels increased without rectification with increasing voltage as evidenced from the current responses to voltage ramps (Fig. 4a). The activity of *xl*-MCC channel increased at more negative potentials (Fig. 4b).

In 35 % of the experiments, single-channel activities of either *i*-MCC or *xl*-MCC were interrupted by a channel with bursting kinetics and periods of high amplitude and frequency of open-closed transitions separated by silent intervals (Fig. 5a). Burst activities were observed either simultaneously with *i*-MCC or *xl*-MCC gating or were a sole type of current activity observed in the particular patch (Fig. 5b). The corresponding amplitude histogram showed that the single-channel amplitude of these burst currents (burst mitochondrial Ca^{2+} channel (*b*-MCC)) at −100 mV was 2.3 pA, corresponding to a conductance of 22.5±1.7 pS (n=10) (Fig. 5c). Similar to *i*-MCC and *xl*-MCC, single-channel activity of *b*-MCC channels increased with increasing voltage (Fig. 6a). Single-channel amplitude of *b*-MCC channels showed no rectification within voltage range from −60 to −140 mV (Fig. 6b).

The open probability (Npo) of *i*-MCC and *xl*-MCC were quite similar and exceeded that of the *b*-MCC by 2-fold (Table 2). In terms of open/close kinetics, the mean open time (To_{mean}) and mean closed time (Tc_{mean}) of the *i*-MCC and *b*-MCC were similar. In contrast, To_{mean} and Tc_{mean} for the *xl*-MCC exceeded that of the other two channels by 10-and 2.5-fold, respectively (Table 2).

Ca^{2+} dependence of the distinct mitoplast (Ca^{2+}) inward currents

In the absence of Ca^{2+} in patch pipettes, no channel activity was observed in nine patches tested (data not shown) at voltages −100 to −150 mV. These observations strongly indicate that the observed channel activities are mediated by Ca^{2+} fluxes.

Sensitivity of the distinct mitoplast (Ca^{2+}) inward currents to RuR

We next explored the sensitivity of the three distinct single-channel activities to RuR, the golden standard of an inhibitor of the mitochondrial Ca^{2+} uniporter. When 1 μM RuR was present in the pipettes, the occurrences of *i*-MCC and *b*-MCC channels were not altered (13 out of 19 patches).

Among these 13 patches, 2 patches exhibited *xl*-MCC activity in the presence of 1 μM RuR, suggesting that the occurrence of *xl*-MCC is also not affected by 1 μM RuR. The conductances of these two *xl*-MCC channels were reduced in the presence of 1 μM RuR in the pipettes to 54 and 48 pS compared with the mean conductance of *xl*-MCC channels of 80.2±7.8 pS (Fig. 7a; Table 3). These observations indicate that the *xl*-MCC conductance, but not occurrence, is reduced in the presence of 1 μM RuR. In the presence of 10 μM RuR in the pipette, the *i*-MCC channel activity was observed in seven out of nine patches tested. Under these conditions, the conductance of *i*-MCC channel was reduced to 7.3±1.1 pS (n=7) (Fig. 7b, c) compared with 11.7±0.6 pS in the absence of RuR. Similar to the *i*-MCC, *b*-MCC conductance was reduced in the presence of 10 μM RuR in the pipette (from 22.6±1.7 pS in the absence of RuR to 16.3±1.8 pS (n=4) in the presence of 10 μM RuR in the pipette) (Table 3). However, among these nine patches tested with 10 μM RuR in the pipette, no *xl*-MCC activity was observed, thus indicating that 10 μM RuR completely prevented *xl*-MCC activity. In the presence of 30 μM RuR in patch pipette, no single-channel activity was observed in 12 patches tested.

We also explored the effect of RuR applied to the bath solution on activities of mitochondria Ca^{2+} channels. When 1 μM RuR was applied to the bath solution the activity but not the conductance of *i*-MCC and *b*-MCC channels was decreased (Fig. 8a). At concentration 10 μM, RuR largely suppressed the single-channel amplitude and open probability (up to 70 %) of both *i*-MCC and *b*-MCC. In two out of six patches, 10 μM RuR applied to the bath completely suppressed the activity of both *i*-MCC and *b*-MCC. The *xl*-MCC activity was largely suppressed by 1 μM RuR and completely inhibited by 10 μM RuR (Fig. 8b). Altogether, these observations may indicate that *i*-MCC and *b*-MCC are less sensitive to RuR than *xl*-MCC (Table 3).

Pharmacological characterization of (Ca^{2+}) inward currents in mitoplasts

As in all experiments described above 10 μM CsA and CGP 37187 were present in the pipette solutions, the observed three mitoplast (Ca^{2+}) currents were obviously not sensitive to inhibition of the PTP, NCX_{mito}, and LETM1.

The inner mitochondrial membrane contains Cl^- channels activated at depolarized but not hyperpolarized voltages [24]. Nevertheless, to exclude the possibility that the observed channel activities were caused by Cl^- conductances, experiments using a pipette solution with a reduced Cl^- concentration (PS2, Table 1) were performed. A decrease of Cl^- concentration either in a pipette (Fig. 9a, b) or a bath (Figs. 8a, b and 9c, d) solution failed to affect inward openings at negative potentials and single-channel conductance. Voltage ramps from −150 to 150 mV revealed single-channel opening events at voltages positive than +30 mV likely corresponding to the activity of Cl^- channels (Fig. 9e). Subsequently, the sensitivity of mitoplast ion currents to well-known Cl^- channel inhibitors has been tested. Neither the presence in the pipette solution of 100 μM niflumic acid, nor 100 μM

DIDS prevented the single-channel activities of *xl*-MCC (Figs. 8b and 10a), *i*-MCC and *b*-MCC (Fig. 10b) suggesting that Cl^- channels unlikely account for the observed single-channel activities (Table 3). Incorporation of either paxilline (1 μM), iberiotoxin (100 nM), or glibenclamide (10 μM) into the patch pipette failed to prevent single-channel activities (Table 3; Fig. 10c).

Discussion

In view of the recent progress in the molecular identification of potential contributors to mitochondrial Ca^{2+} uptake (MCU [3, 6], RyR1 [22], LETM 1 [12, 28], and UCP2/3 [25, 26]) and the remaining evaluation of the individual contributions of these proteins to mitochondrial Ca^{2+} signaling in situ, there is an emerging need for a biophysical and pharmacological characterization of these co-existing Ca^{2+} channels of the inner mitochondrial membrane. Our work for the first time provides a clear and transparent basis for studying Ca^{2+} currents of the inner mitochondrial membrane that will help to identify and characterize possible contributors of mitochondrial Ca^{2+} uptake on the molecular level.

Our findings that the currents measured required Ca^{2+} in the pipette indicate that all currents indeed represent Ca^{2+} conductances through the inner mitochondrial membrane. This assumption was further supported by our findings that under conditions in which only Ca^{2+} and Cl^- were present (i.e., PS1) in the pipette/mitoplast matrix, the Cl^- channel blockers DIDS and niflumic acid, and the K^+ channel inhibitors paxilline, iberiotoxin, and glibenclamide did not affect the individual currents. In line with these findings, a reduced Cl^- content of either the pipette or bath buffer did not affect the individual currents. Overall, these data indicate that the three currents described above most likely represent three distinct Ca^{2+} conductances across the inner mitochondrial membrane.

The *xl*-MCC channel activity was observed inconsistently and their occurrence varied between different experimental days. Hence, it was difficult to consistently conduct experiments specifically on this channel type. In regard of possible channels with similar characteristics to those described above, we cannot completely exclude possible contamination of mitochondrial fractions from the plasma membrane sheets. Cell fractionation has become a standard procedure combining various centrifugation steps and purity of mitoplasts was tested by Western blotting of respective proteins. Moreover, because electrophysiological recordings from mitoplasts were preceded by mitoplast selection and chasing with the patch pipette under visual control, measurements of proteins from other cellular compartments are highly unlikely, although not absolutely excludable.

In the present study we show that under conditions that facilitate Ca^{2+} currents, mitoplasts isolated from HeLa cells exhibit three distinct types of single-channel activity: most frequently an 11 pS channel (*i*-MCC) was observed. In addition, a burst-channel with conductance of 23 pS (*b*-MCC) and a rare, large channel with a conductance of 80 pS (*xl*-MCC) were recorded. The co-existence of *i*-MCC and *xl*-MCC in mitoplasts form HeLa cells is in line with our previous report [11]. Hence, the conductance of *i*-MCC, channel density, and its gating characteristics found in mitoplasts from HeLa cells (this paper) and endothelial cells [11], obviously correspond to the mCa1 entitled current recorded in cardiac myocytes [17], thus, pointing to *i*-MCC as to be a likely candidate for an ubiquitous Ca^{2+} channel of the inner mitochondrial membrane. However, with its conductance between 11 and 14 pS, *i*-MCC exceeds that of MCU reconstituted into planar lipid bilayer (6–7 pS) [6], the most promising candidate representing the pore-forming unit of a mitochondrial Ca^{2+} channel [3, 6].

Europe PMC Funders Author Manuscripts

However, a conductance (i.e., 3–8 pS) very similar to that found in planar lipid bilayer with reconstituted MCU was recorded from mitoplasts isolated from COS7 cells [13], cardiac myocytes (mCa2) [17], and endothelial cells (*s*-MCC) [11] but not in HeLa cells (this study and [11]). This is particular notable as MCU is expressed in HeLa cells and was functionally characterized in this particular cell type [3, 6]. Recently, MICU1 [19] was described as a gatekeeping modulator protein regulating the MCU activity [15], thus, this discrepancy might be due to the lack of MICU1 in the in vitro experimental setup, resulting in the channel activity with reduced conductance when measurements are performed from planar lipid bilayer with reconstituted MCU. Accordingly, the individual contribution of MCU and other putative Ca^{2+} channels/carriers of the mitochondrial inner membrane (i.e., Letm1, RyR1, and UCP2/3 [14, 18]) to the three Ca^{2+} currents described herein remains speculative and essentially awaits further investigation.

Moreover, at the current stage, it is unclear whether or not the three distinct types of channel activities we found in the inner mitochondria membrane of HeLa cells correlate with distinct ion carrier proteins of the inner mitochondrial membrane. We also cannot exclude the possibility that during mitoplast preparation procedure certain proteins that normally reside in the outer mitochondrial membrane (e.g., VDAC [2, 23] or mitofusin-2 [1, 5, 16]) interact with the Ca^{2+} channels of the inner mitochondrial membrane and, subsequently, affect their conductances and biophysical behavior. Hence, the different conductances observed might be either a feature of three distinct Ca^{2+} transport proteins of the inner mitochondrial membrane, or represent different conductance states of one single channel that might be influenced by interactions with proteins of the outer mitochondrial membrane. In this regard, it remains unclear whether or not *b*-MCC indeed represents an independent single-type channel or the burst current activity reflects a not fully open state of the *xl*-MCC channel.

Due to the individual sensitivities to RuR and the different conductances, it is tempting to speculate that *xl*-MCC, *b*-MCC and *i*-MCC are indeed distinct Ca^{2+} channels in one given mitochondrion. Notably, *xl*-MCC was found to be more sensitive to RuR than *i*-MCC and *b*-MCC, thus, pointing to some similarities between *i*-MCC and *b*-MCC. In spite of the huge Ca^{2+} gradient the reversal potential for all three Ca^{2+} currents was quite low, most likely indicating that free Ca^{2+} concentration into the mitochondria matrix was quite high. Importantly, we performed experiments in Na^+ free bath solution, which prevents Ca^{2+} extrusion from mitoplasts via NCX_{mito}.

In the present work, three distinct types of Ca^{2+} currents through the inner mitochondrial membrane have been described that essentially depend on transmembrane Ca^{2+} movements and are neither sensitive to inhibitors of Cl^- and K^+ channels nor susceptible to an inhibition of the PTP, Letm1 and the NCX_{mito}. Based on their individual biophysical characteristics and sensitivity to RuR, these currents are most likely established by three distinct channels/complexes, thus, challenging the view of a unique, ubiquitous mitochondrial Ca^{2+} uniporter. Applying the experimental procedures presented herein, studies on the individual contribution of the reported putative mitochondrial Ca^{2+} channel/carrier proteins to the distinct Ca^{2+} currents across the inner mitochondrial membrane appear feasible.

Acknowledgments

We thank Therese Macher, Rene Rost, Ph.D., and Florian Enzinger for their excellent technical assistance. This work was supported by the Austrian Science Funds (FWF, P20181-B05 P21857-B18 and P22553-B18). C.J.-Q. is a fellow of the Doctoral College “Metabolic and Cardiovascular Disease”, funded by the Austrian Science Fund (FWF W1226-B18) and the Medical University of Graz, the University of Graz and the Graz University of Technology.

References

1. Bach D, Pich S, Soriano FX, Vega N, Baumgartner B, Oriola J, Daugaard JR, Lloberas J, Camps M, Zierath JR, Rabasa-Lhoret R, Wallberg-Henriksson H, Laville M, Palacin M, Vidal H, Rivera F, Brand M, Zorzano A. Mitofusin-2 determines mitochondrial network architecture and mitochondrial metabolism. A novel regulatory mechanism altered in obesity. J Biol Chem. 2003; 278:17190–17197. [PubMed: 12598526]
2. Bahamonde MI, Valverde MA. Voltage-dependent anion channel localises to the plasma membrane and peripheral but not perinuclear mitochondria. Pflugers Arch. 2003; 446:309–313. [PubMed: 12698369]
3. Baughman JM, Perocchi F, Girgis HS, Plovanich M, Belcher-Timme CA, Sancak Y, Bao XR, Strittmatter L, Goldberger O, Bogorad RL, Koteliansky V, Mootha VK. Integrative genomics identifies MCU as an essential component of the mitochondrial calcium uniporter. Nature. 2011; 476:341–345. [PubMed: 21685886]
4. Bernardi P, Vassanelli S, Veronese P, Colonna R, Szabo I, Zoratti M. Modulation of the mitochondrial permeability transition pore. Effect of protons and divalent cations. J Biol Chem. 1992; 267:2934–2939. [PubMed: 1737749]
5. de Brito OM, Scorrano L. Mitofusin 2 tethers endoplasmic reticulum to mitochondria. Nature. 2008; 456:605–610. [PubMed: 19052620]
6. De Stefani D, Raffaello A, Teardo E, Szabò I, Rizzuto R. A forty-kilodalton protein of the inner membrane is the mitochondrial calcium uniporter. Nature. 2011; 476:336–340. [PubMed: 21685888]
7. Duchen MR. Mitochondria and Ca^{2+} in cell physiology and pathophysiology. Cell Calcium. 2000; 28:339–348. [PubMed: 11115373]
8. Frezza C, Cipolat S, Scorrano L. Organelle isolation: functional mitochondria from mouse liver, muscle and cultured fibroblasts. Nat Protoc. 2007; 2:287–295. [PubMed: 17406588]
9. Graier WF, Frieden M, Malli R. Mitochondria and Ca^{2+} signaling: old guests, new functions. Pflugers Arch. 2007; 455:375–396. [PubMed: 17611770]
10. Hagen T, Lagace CJ, Modica-Napolitano JS, Aprille JR. Permeability transition in rat liver mitochondria is modulated by the ATP-Mg/Pi carrier. Am J Physiol. 2003; 285:G274–G281.
11. Jean-Quartier C, Bondarenko AI, Alam MR, Trenker M, Waldeck-Weiermair M, Malli R, Graier WF. Studying mitochondrial Ca^{2+} uptake—a revisit. Mol Cell Endocrinol. 2012; 353:114–127. [PubMed: 22100614]
12. Jiang D, Zhao L, Clapham DE. Genome-wide RNAi screen identifies LETM1 as a mitochondrial Ca^{2+}/H^{+} antiporter. Science. 2009; 326:144–147. [PubMed: 19797662]
13. Kirichok Y, Krapivinsky G, Clapham DE. The mitochondrial calcium uniporter is a highly selective ion channel. Nature. 2004; 427:360–364. [PubMed: 14737170]
14. Malli R, Graier WF. Mitochondrial Ca^{2+} channels: great unknowns with important functions. FEBS Lett. 2010; 584:1942–1947. [PubMed: 20074570]
15. Mallilankaraman K, Doonan P, Cárdenas C, Chandramoorthy HC, Müller M, Miller R, Hoffman NE, Gandhirajan RK, Molgó J, Birnbaum MJ, Rothberg BS, Mak D-OD, Foskett JK, Madesh M. MICU1 is an essential gatekeeper for MCU-mediated mitochondrial Ca^{2+} uptake that regulates cell survival. Cell. 2012; 151:630–644. [PubMed: 23101630]
16. Merkwirth C, Langer T. Mitofusin 2 builds a bridge between ER and mitochondria. Cell. 2008; 135:1165–1167. [PubMed: 19109886]
17. Michels G, Khan IF, Endres-Becker J, Rottlaender D, Herzig S, Ruhparwar A, Wahlers T, Hoppe UC. Regulation of the human cardiac mitochondrial Ca^{2+} uptake by 2 different voltage-gated Ca^{2+} channels. Circulation. 2009; 119:2435–2443. [PubMed: 19398664]
18. Pan S, Ryu SY, Sheu SS. Distinctive characteristics and functions of multiple mitochondrial Ca^{2+} influx mechanisms. Sci China Life Sci. 2011; 54:763–769. [PubMed: 21786199]
19. Perocchi F, Gohil VM, Girgis HS, Bao XR, McCombs JE, Palmer AE, Mootha VK. MICU1 encodes a mitochondrial EF hand protein required for Ca^{2+} uptake. Nature. 2010; 467:291–296. [PubMed: 20693986]

20. Ruiz-Meana M, Garcia-Dorado D, Miró-Casas E, Abellán A, Soler-Soler J. Mitochondrial Ca^{2+} uptake during simulated ischemia does not affect permeability transition pore opening upon simulated reperfusion. Cardiovasc Res. 2006; 71:715–724. [PubMed: 16860295]
21. Ryu SY, Beutner G, Dirksen RT, Kinnally KW, Sheu S-S. Mitochondrial ryanodine receptors and other mitochondrial Ca^{2+} permeable channels. FEBS Lett. 2010; 584:1948–1955. [PubMed: 20096690]
22. Ryu SY, Beutner G, Kinnally KW, Dirksen RT, Sheu S-S. Single channel characterization of the mitochondrial ryanodine receptor in heart mitoplasts. J Biol Chem. 2011; 286:21324–21329. [PubMed: 21524998]
23. Shoshan-Barmatz V, Israelson A, Brdiczka D, Sheu SS. The voltage-dependent anion channel (VDAC): function in intracellular signalling, cell life and cell death. Curr Pharm Des. 2006; 12:2249–2270. [PubMed: 16787253]
24. Tomaskova Z, Ondrias K. Mitochondrial chloride channels—what are they for? FEBS Lett. 2010; 584:2085–2092. [PubMed: 20100478]
25. Trenker M, Fertschai I, Malli R, Graier WF. UCP2/3—likely to be fundamental for mitochondrial Ca^{2+} uniport. Nat Cell Biol. 2008; 10:1237–1240.
26. Trenker M, Malli R, Fertschai I, Levak-Frank S, Graier WF. Uncoupling proteins 2 and 3 are fundamental for mitochondrial Ca^{2+} uniport. Nat Cell Biol. 2007; 9:445–452. [PubMed: 17351641]
27. Waldeck-Weiermair M, Duan X, Naghdi S, Khan MJ, Trenker M, Malli R, Graier WF. Uncoupling protein 3 adjusts mitochondrial Ca^{2+} uptake to high and low Ca^{2+} signals. Cell Calcium. 2010; 48:288–301. [PubMed: 21047682]
28. Waldeck-Weiermair M, Jean-Quartier C, Rost R, Khan MJ, Vishnu N, Bondarenko AI, Imamura H, Malli R, Graier WF. The leucine zipper EF hand-containing transmembrane protein 1 (LETM1) and uncoupling proteins-2 and 3 (UCP2/3) contribute to two distinct mitochondrial Ca^{2+} uptake pathways. J Biol Chem. 2011; 286:28444–28455. [PubMed: 21613221]
29. Waldeck-Weiermair M, Malli R, Naghdi S, Trenker M, Kahn MJ, Graier WF. The contribution of UCP2 and UCP3 to mitochondrial Ca^{2+} uptake is differentially determined by the source of supplied Ca^{2+} Cell Calcium. 2010; 47:433–440. [PubMed: 20403634]

Europe PMC Funders Author Manuscripts

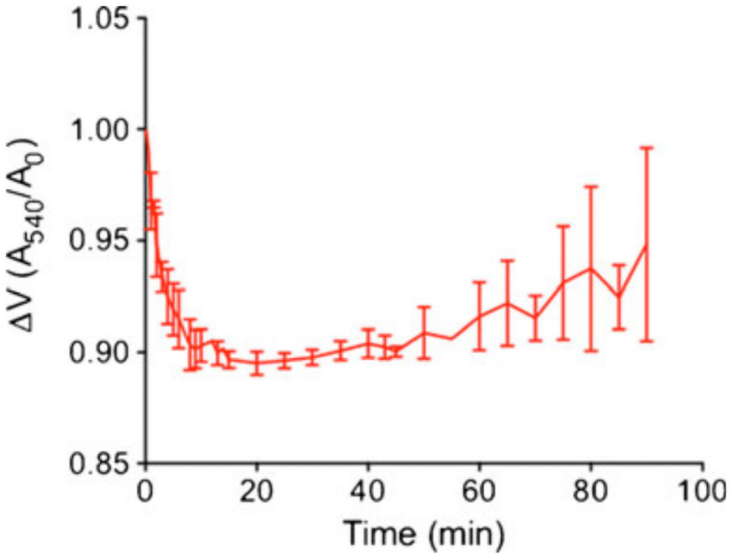

Fig. 1.

Time course of mitochondria swelling in hypotonic solution. Isolated mitochondria were suspended in hypotonic solution (5 mM HEPES, 5 mM sucrose, and 1 mM EGTA pH adjusted to 7.4 with KOH) and volume change due to mitochondrial swelling was monitored as decline in absorbance at 540 nm. Data are expressed as ratio between the change in absorbance over time divided by the absorbance at the initial timepoint (mean±SD, n=3)

Europe PMC Funders Author Manuscripts

Europe PMC Funders Author Manuscripts

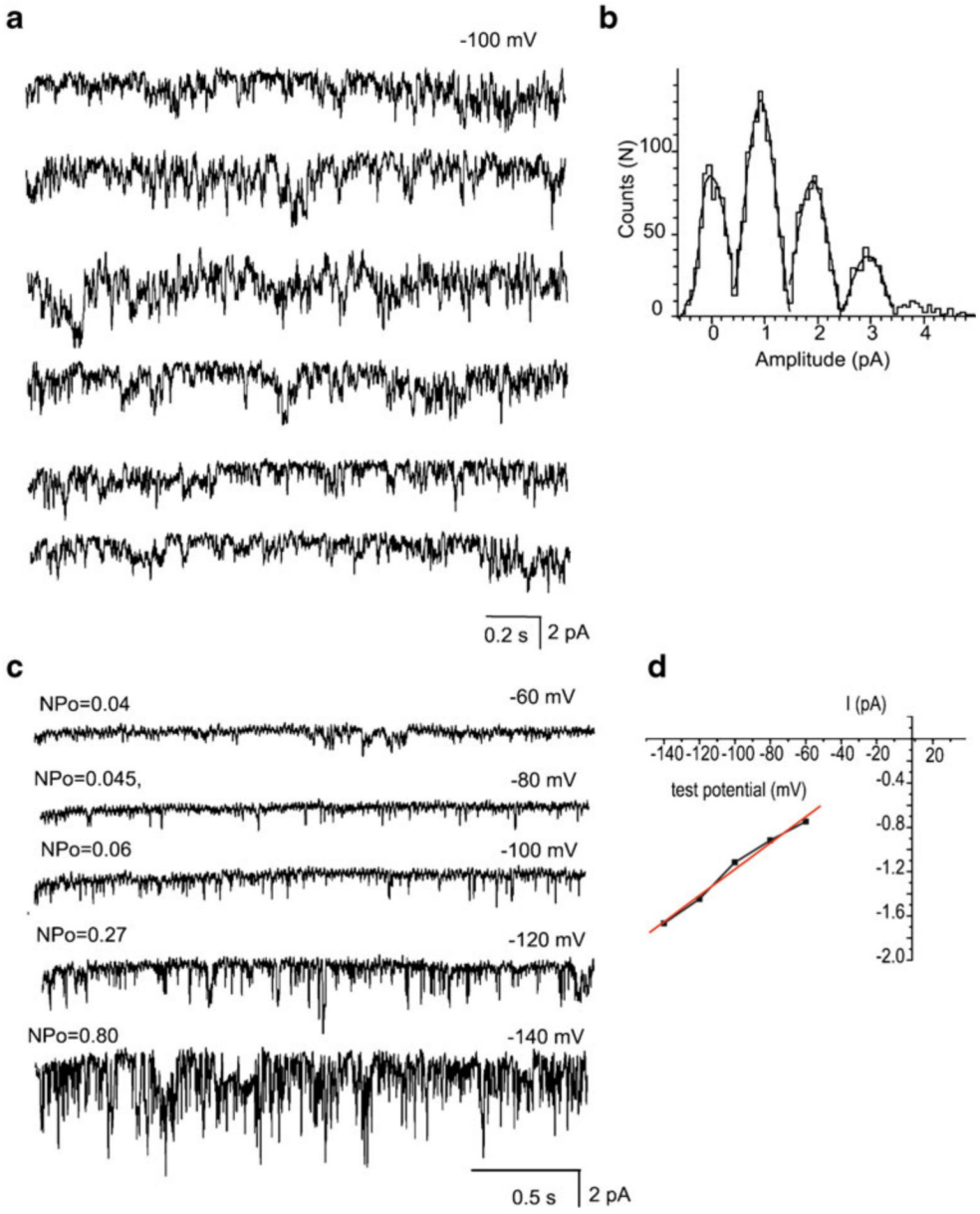

Fig. 2.

i-MCC are present in mitoplasts isolated from HeLa cells. **a** Exemplary traces of *i*-MCC from HeLa mitochondria at test potential of −100 mV. **b** Corresponding amplitude histogram constructed from traces shown in (**a**). **c** *i*-MCC channel activities at different voltages indicated. **d** Corresponding IV curve of the channel activity shown in (**c**)

Europe PMC Funders Author Manuscripts

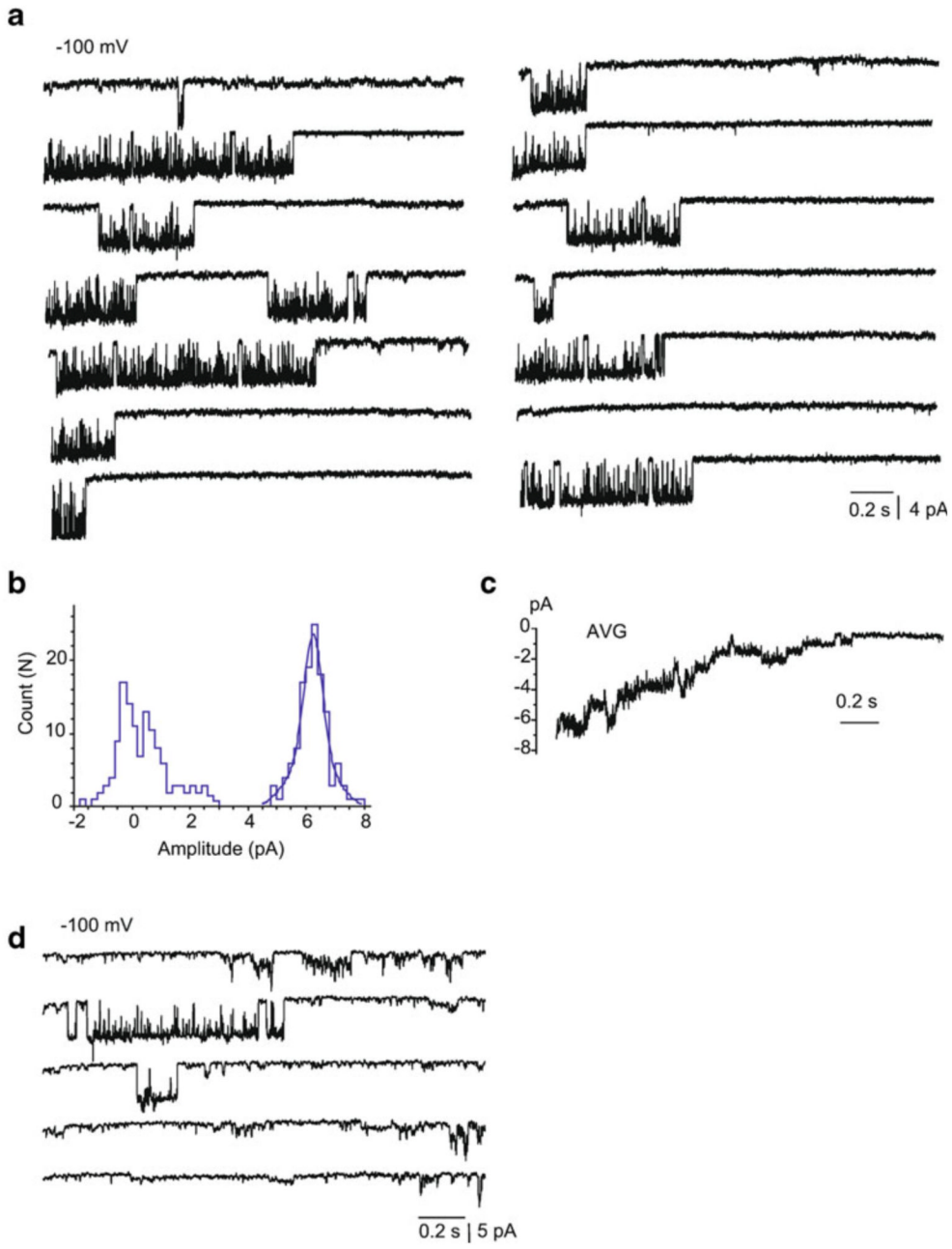

Fig. 3.

xl-MCC are present in mitochondria from HeLa cells. **a** Representative tracings of single-channel events at a test potential of −100 mV showing activity of *xl*-MCC. **b** Corresponding amplitude histogram constructed from traces shown in (**a**). **c** Average of individual traces shown in (**a**). **d** An exemplary recording from HeLa mitoplast showing coexistence of channels with bursting activity, *i*-MCC and *xl*-MCC in the same patch

Europe PMC Funders Author Manuscripts

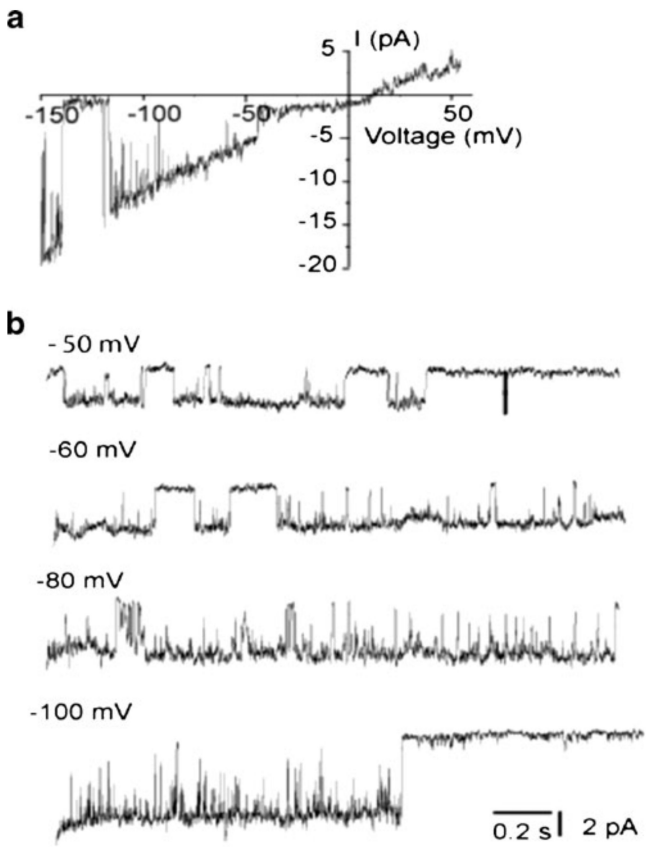

Fig. 4.

Voltage dependency of extra-large conductance Ca^{2+} channel. **a** Representative current traces in response to voltage ramps from −150 to +50 mV showing single-channel activity of *xl*-MCC. The figure depicts the net current obtained after subtraction of the background current obtained from the same patch during nonresponsive sweeps from the *xl*-MCC current responses. **b** *xl*-MCC activity at different voltages indicated

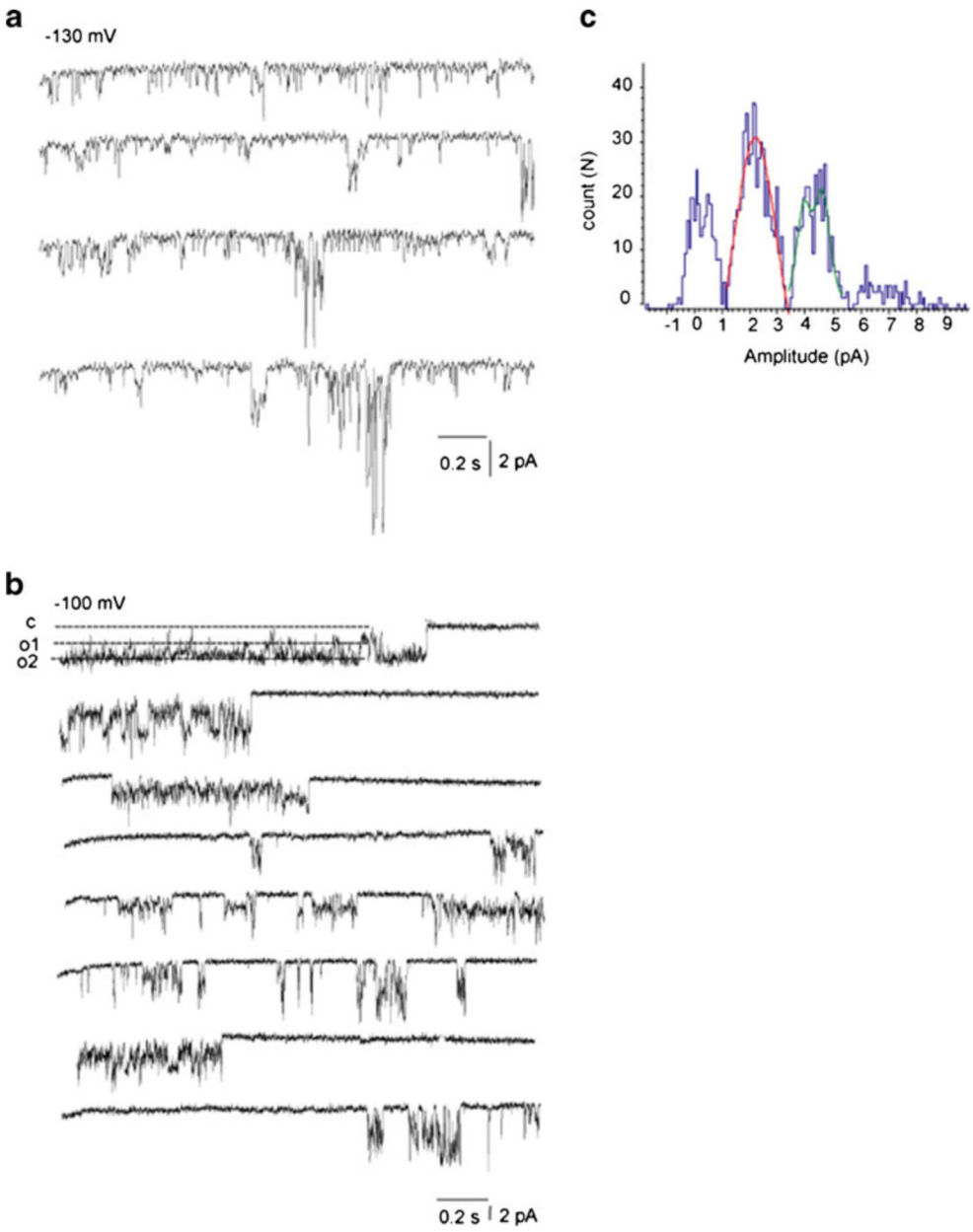

Fig. 5.

Channels with *b*-MCC isolated from HeLa cells. **a** Exemplary traces showing the activity of intermediate conductance mitochondrial Ca^{2+} channels together with bursting channel activity in the same patch. **b** Exemplary traces showing the activity of bursting channel as a sole single-channel activity type. **c** Corresponding amplitude histogram constructed from traces shown in (**b**)

Europe PMC Funders Author Manuscripts

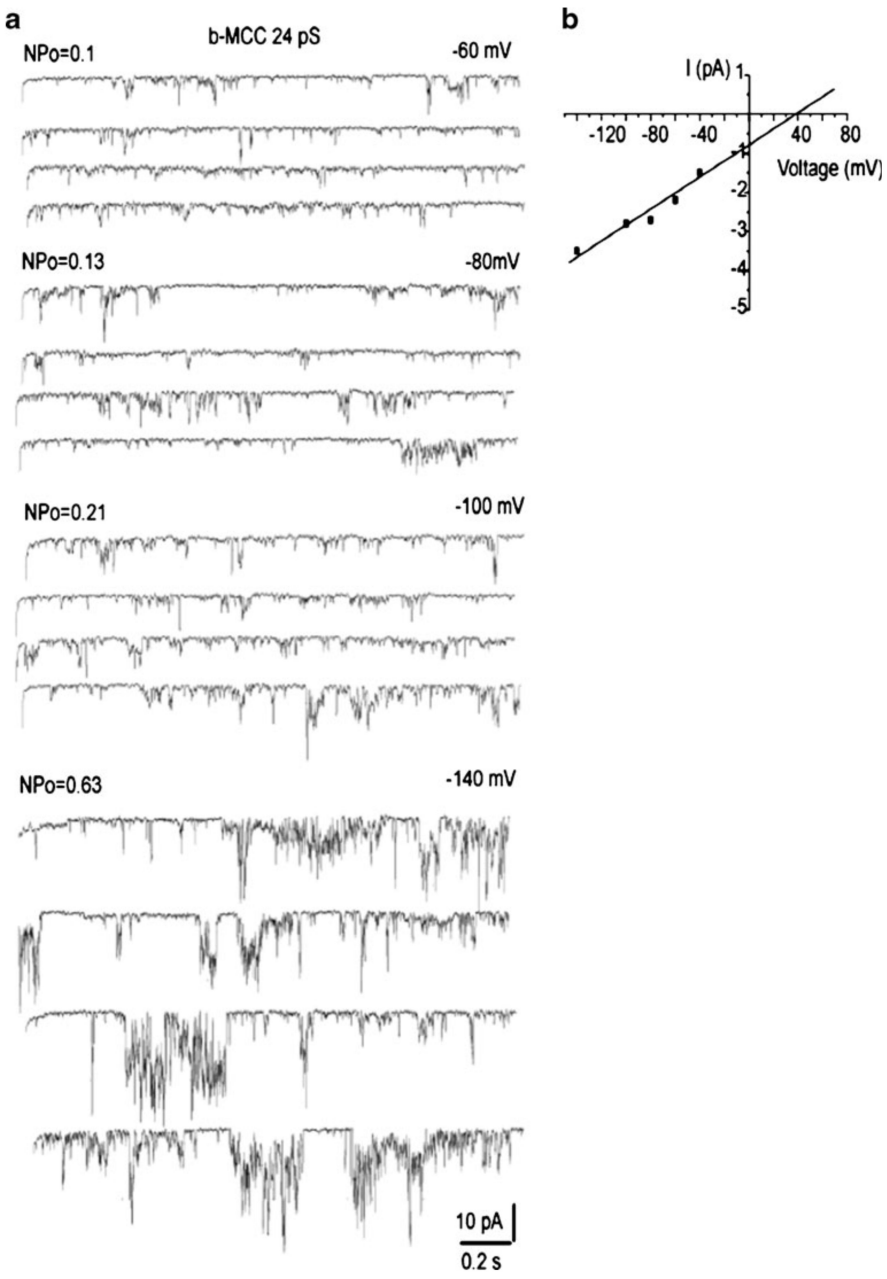

Fig. 6.

Bursting Ca channels (*b-MCC*) are voltage dependent. **a** Exemplary single-channel traces of *b*-MCC at different voltages indicated. Note an increase in the *b*-MCC activity at more negative voltages. **b** Corresponding current–voltage relationship of *i*-MCC

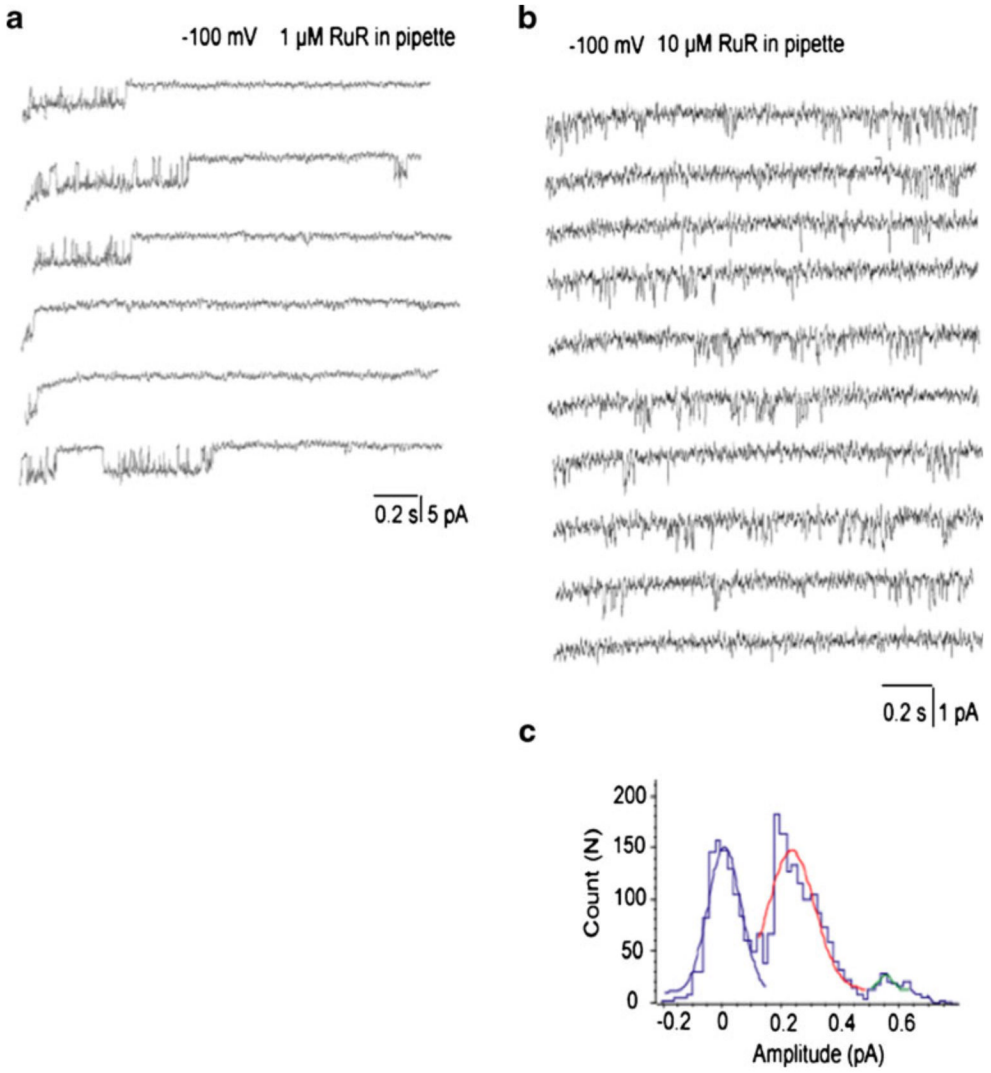

Fig. 7.

Pharmacological inhibition of mitochondrial Ca^{2+} channels by ruthenium red (*RuR*). **a** Exemplary traces showing a decreased unitary amplitude of *xl*-MCC channels in the presence of 1 μM RuR in the pipette. Test potential is −100 mV. **b** Exemplary traces showing reduced single-channel amplitude of *i*-MCC channel activity by 10 μM RuR present in the pipette solution. Standard 105 mM $CaCl_2$-containing solutions was supplemented with 100 μM DIDS, 10 μM CsA, 10 μM CGP 37187, and 10 μM RuR. Test potential is −100 mV. **c** Corresponding amplitude histogram of the channel activity shown in (**b**) reveals decreased single-channel amplitude of *i*-MCC in the presence of RuR

Europe PMC Funders Author Manuscripts

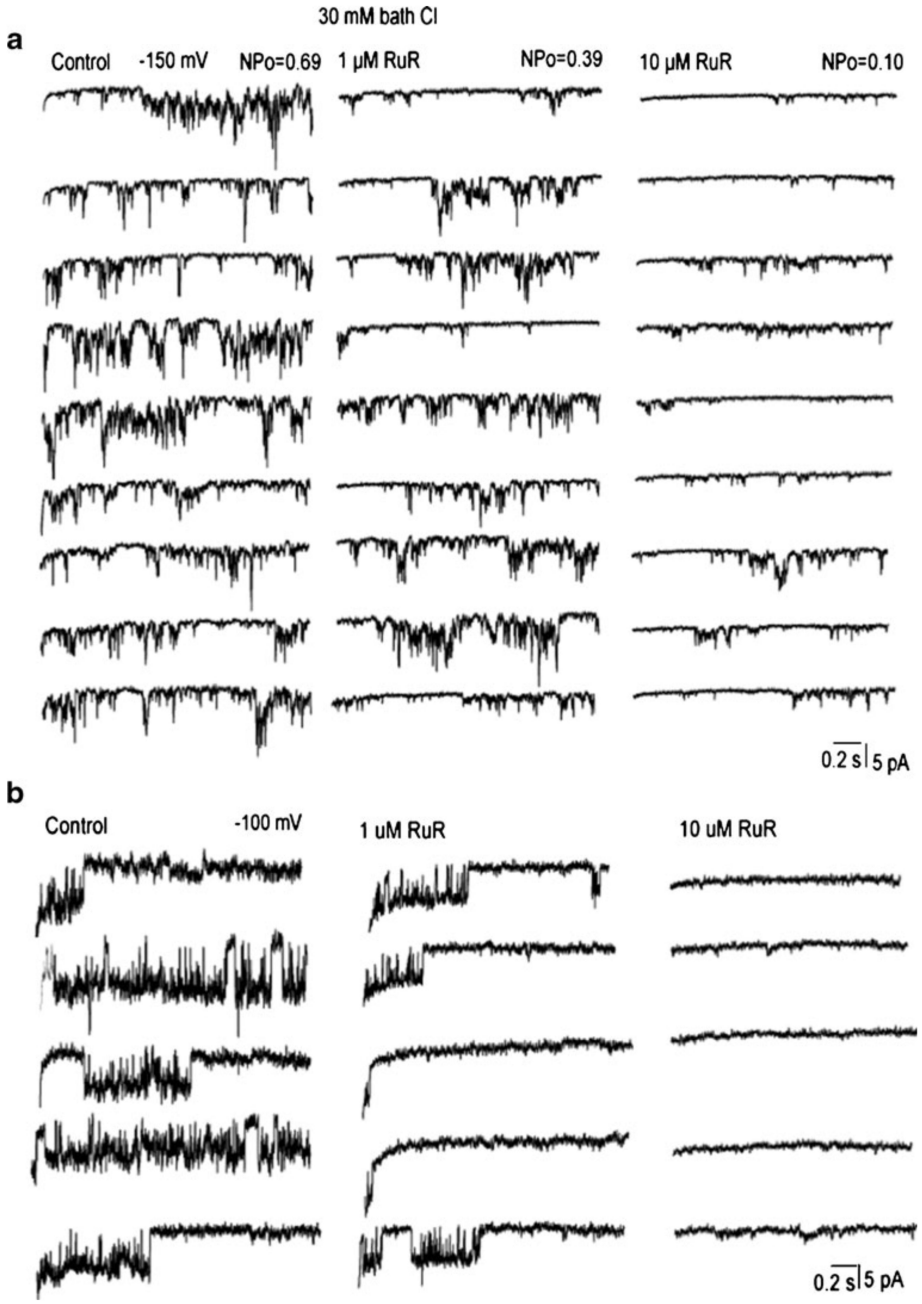

Fig. 8.

Ruthenium red suppresses the activities of mitochondrial Ca^{2+} channels. **a**, **b** Representative traces showing the activities of *b*-MCC at test potential of −150 mV (**a**) and *xl*-MCC at test potential of −100 mV (**b**) before (control) and after addition of 1 and 10 μM RuR into the bath solution. Recordings were performed in the bath solution containing 40 mM Cl^- in the absence (**a**) and presence (**b**) of 100 μM DIDS in the pipette solution

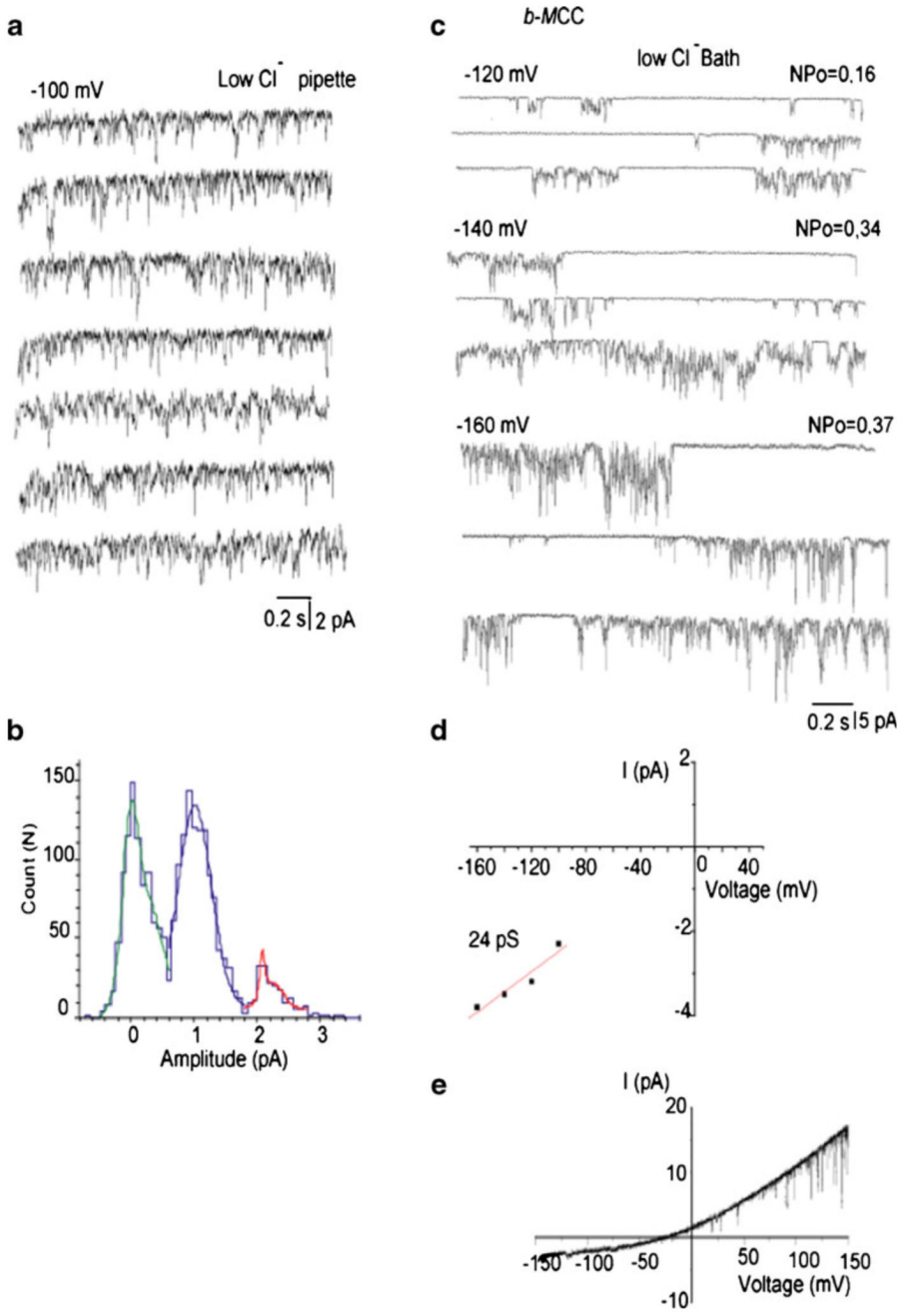

Fig. 9.

Effect of manipulation of Cl^- concentrations on (Ca^{2+}) inward currents in mitoplasts. **a** Representative traces of *i*-MCC channel activity recorded with the use of low Cl^- (40 mM Cl^-)-containing pipette solution. Test potential is −100 mV. **b** Amplitude histogram of the channel activity shown in (**a**). **c** Representative traces showing the activity of *b*-MCC at different voltages indicated in the presence of 40 mM bath Cl^-. **d** Corresponding voltage dependency of single-channel amplitudes of single-channel openings shown in (**c**). **e** Representative current responses to a voltage ramps from −150 to +150 mV under our standard recording conditions showing the activity of Cl^- channels at positive potentials

Europe PMC Funders Author Manuscripts

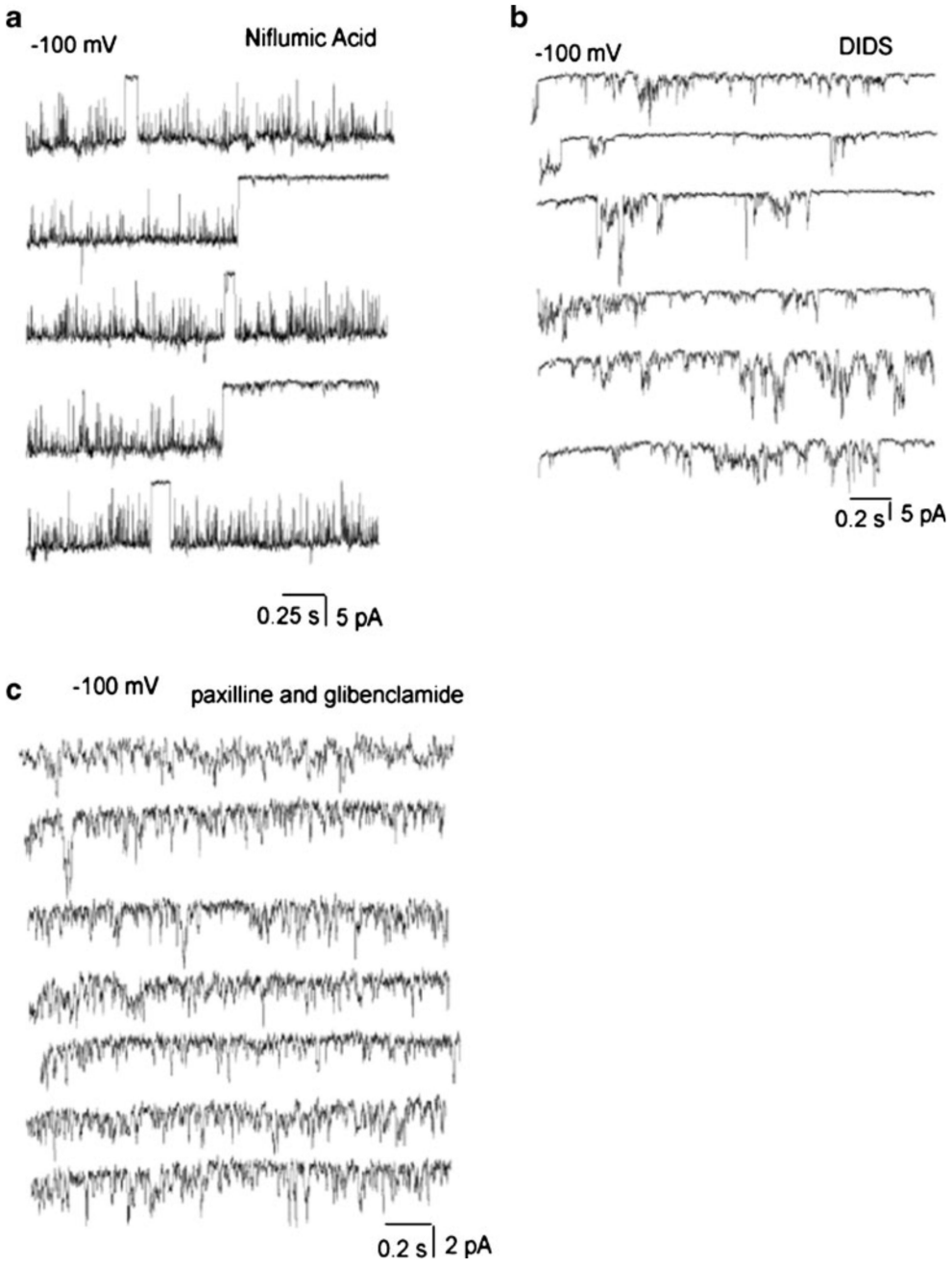

Fig. 10.

Pharmacological characterization of (Ca^{2+}) inward currents in mitoplasts. **a** Representative traces showing *xl*-MCC channel activity in the presence of 100 μM niflumic acid in the pipette solution. Test potential is −100 mV. **b** Representative traces showing the activities of *b*-MCC and *i*-MCC in the same patch in the presence of 100 μM DIDS in the pipette solution. Test potential is −100 mV. **c** Representative traces showing the activity of *b i*-MCC in the presence of 1 μM paxilline and 10 μM glibenclamide in the pipette solution. Test potential is −100 mV

Table 1

Composition of pipette solutions (PS) used to detect mitoplast Ca^{2+} currents in the mitoplast-attached configuration

	Composition of pipette solution (mM)	Appearance of *i*-MCC	Appearance of *xl*-MCC
PS1	105 $CaCl_2$	Yes	Yes
	10 HEPES		
	0.01 CsA		
	0.01 CGP 37187		
PS2	65 Ca MeS	Yes	Yes
	40 $CaCl_2$		
	10 HEPES		
	0.01 CsA		
	0.01 CGP 37187		
PS3	220 sucrose	No	No
	35 NMDG-Cl		
	10 HEPES		
	2 EGTA		
	0.1 DIDS		
	0.01 CsA		
	0.01 CGP 37187		

The pH of all solutions was adjusted to 7.2 with KOH. In all experiments, bath solution contained (in millimolars): 150 KCl, 1 EGTA, 1 EDTA, 10 HEPES, pH was adjusted to 7.2 with KOH

Europe PMC Funders Author Manuscripts

Table 2

Gating characteristics of the detected mitoplast Ca^{2+} currents

	NPo(ms)	Tc_{mean}	To_{mean}(ms)	Number
i-MCC	0.61±0.14	3.5±0.5	14.9±2.4	13
xl-MCC	0.77±0.06	45.8±14.3	57.7±15.9	8
b-MCC	0.34±0.08	4.4±0.9	22.6±2.6	5

In all experiments, bath solution contained (in mM): 150 KCl, 1 EGTA, 1 EDTA, and 10 HEPES and pH was adjusted to 7.2 with KOH. Open probability (NPo), mean open time (To_{mean}) and mean close time (Tc_{mean}) of intermediate (*i*-MCC), extra-large mitochondrial Ca^{2+} channel (*xl*-MCC) and burst (*b*-MCC) mitochondrial Ca^{2+} channels are presented as means ± SEM. n, provides the number of individual patches for the respective experiments

Europe PMC Funders Author Manuscripts

Table 3

Overview on the pharmacological profile of mitoplast Ca^{2+} currents

Target	Compound to be tested (M)	Concentration	Inhibition of *i*-MCC	Inhibition of *xl*-MCC	Inhibition of *b*-MCC
MCU	Ruthenium red	1	None	Moderate	None
		10	Moderate	Strong	Moderate
		30	Strong	Strong	Strong
NCX_{mito}	CGP 37187	10	None	None	None
PTP	Cyclosporin A	10	None	None	None
(B)K_{Ca}	Paxilline IbTX	1 0.1	None	None	None
			None	None	None
K_{ATP}	Glibenclamide	10	None	None	None
Cl channels	DIDS	100	None	None	None
Nonselective cation channels	Niflumic acid	100	None	None	None

The inhibitory potential of the compounds on *i*-MCC, *xl*-MCC, and *b*-MCC were evaluated in experiments using PS1 and PS2 in the pipette. Experiments were performed in mitoplasts of at least five different isolation days.Mitoplasts were isolated from HeLa cells as described under “Materials and methods”